

Kinetic Analysis of the Binding of Human Matrix Metalloproteinase-2 and -9 to Tissue Inhibitor of Metalloproteinase (TIMP)-1 and TIMP-2*

(Received for publication, June 6, 1997, and in revised form, September 2, 1997)

Matthew W. Olson^{‡§}, David C. Gervasi^{‡§}, Shahriar Mobashery[¶], and Rafael Fridman^{‡§||}

From the [‡]Department of Pathology and the [§]Karmanos Cancer Institute and [¶]Department of Chemistry, Wayne State University, Detroit, Michigan 48201

The dissociation constants (K_d) of tissue inhibitor of metalloproteinase (TIMP)-1 and TIMP-2 for the active and latent forms of matrix metalloproteinase (MMP)-2 and MMP-9 were evaluated using surface plasmon resonance (SPR) and enzyme inhibition studies. SPR analysis shows biphasic kinetics with high (nM) and low (μ M) affinity binding sites of TIMP-2 and TIMP-1 for MMP-2 (72- and 62-kDa species) and MMP-9 (92- and 82-kDa species), respectively. In contrast, binding data of TIMP-2 to an MMP-2 45-kDa active form lacking the C-terminal domain and to an MMP-2 C-terminal domain (CTD) fragment displays monophasic kinetics with K_d values of 315 and 60 nM, respectively. This suggests that the CTD contains the high affinity binding site, whereas the catalytic domain contains the low affinity site. Also, binding of TIMP-2 to pro-MMP-2 is stronger at both the high and low affinity sites than the corresponding binding of TIMP-2 to the MMP-2 62-kDa form demonstrating the importance of the N-terminal prodomain. In addition, the K_d value of TIMP-1 for the MMP-2 62-kDa species is 28.6 nM at the high affinity site, yet neither the MMP-2 45-kDa species nor the CTD interacts with TIMP-1. Enzyme inhibition studies demonstrate that TIMPs are slow binding inhibitors with monophasic inhibition kinetics. This suggests that a single binding event results in enzyme inhibition. The kinetic parameters for the onset of inhibition are fast ($k_{on} \sim 10^5 \text{ M}^{-1} \text{ s}^{-1}$) with slow off rates ($k_{off} \sim 10^{-3} \text{ s}^{-1}$). The inhibition constants (K_i) are in the 10^{-7} – 10^{-9} M range and correlate with the values determined by SPR.

The gelatinases MMP-2 (gelatinase A) and MMP-9 (gelatinase B) are two members of the MMP¹ family, a group of zinc-dependent endopeptidases known to hydrolyze many components of the extracellular matrix (1). Like other MMPs, the gelatinases are produced in a latent form (pro-MMP) requiring activation and are inhibited by TIMPs (1–3). A unique characteristic of the gelatinases is the ability of their zymogens to form tight non-covalent and stable complexes with TIMPs. It

has been shown that pro-MMP-2 binds TIMP-2 (4), whereas pro-MMP-9 binds TIMP-1 (5). Although the physiological significance of the proenzyme-inhibitor complex is not completely understood, the complex may play a role in zymogen stabilization and activation (6–8). The interactions of TIMP-2 with pro-MMP-2 and of TIMP-1 with pro-MMP-9 were previously examined by analysis of enzyme activity using truncated enzymes and inhibitors (9–11). These studies demonstrated that the CTD of gelatinases increases the rate of association of the TIMPs for the active enzymes. Studies with activated and C-terminally truncated enzymes demonstrated that the catalytic domain is also involved in TIMP binding (9, 11). However, to date, no quantitative binding analyses of TIMP-1 or TIMP-2 for the latent forms of MMP-2 and MMP-9 have been described. We report herein the first such quantitative binding analysis by surface plasmon resonance (SPR) using highly purified recombinant enzymes and inhibitors (for reviews of SPR see Refs. 12–14). In addition, we report a quantitative analysis of the affinities of TIMP-1 and TIMP-2 for the active forms of either MMP-2 or MMP-9 both in the presence and absence of a substrate. These studies quantitatively define the nature of the unique interactions of MMP-2 and MMP-9 forms with TIMP-1 and TIMP-2.

EXPERIMENTAL PROCEDURES

Buffers—Buffer B (10 mM sodium acetate (pH 4.5)), buffer W (7.8 mM NaH_2PO_4 , 8 mM Na_2HPO_4 (pH 7.2), 137 mM NaCl, 0.1 mM CaCl_2 , 3 mM KCl, 1.5 mM KH_2PO_4 , and 0.02% Tween 20), buffer C (50 mM Tris (pH 7.5), 150 mM NaCl, 5 mM CaCl_2 , 0.02% Brij-35), buffer HA (25 mM Tris (pH 7.5), 25 mM NaCl, and 0.02% Brij-35), buffer R (50 mM Tris (pH 7.5), 5 mM CaCl_2 , 0.01% Brij-35), and phosphate-buffered saline (10 mM NaPO_4 (pH 7.2), 150 mM NaCl) were used.

Proteins and Enzymes—Molecular weight marker proteins for SDS-PAGE were purchased from Bio-Rad. Human recombinant stromelysin 1 was the generous gift of Dr. Paul Cannon (Center for Bone and Joint Research, Palo Alto, CA). A recombinant C-terminal fragment of human MMP-2, comprising amino acids 440–660 (15), was the generous gift of Dr. G. I. Goldberg (Washington University, St. Louis, MO).

Chromatographic Supports—Gelatin-agarose (4% cross-linked), heparin-agarose, Reactive Red 120-agarose, and lectin lentil-Sepharose 4B were purchased from Sigma. A Resource S column and Sephadex-G50 (fine) were purchased from Pharmacia Biotech Inc.

Expression and Purification of Gelatinases and TIMPs—Human pro-MMP-2, pro-MMP-9, and their inhibitors TIMP-1 and TIMP-2 were expressed in a recombinant vaccinia virus mammalian cell expression system, as described earlier (16). Pro-MMP-2 and pro-MMP-9 were purified to homogeneity from the media of infected HeLa cells by gelatin-agarose chromatography, as described previously (16). The protein concentrations of pro-MMP-2 and pro-MMP-9 were determined using their molar extinction coefficients of 122,800 and 114,360 $\text{M}^{-1} \text{ cm}^{-1}$, respectively (2). The MMP-2 45-kDa active form was isolated as described (17). The MMP-2 62-kDa species was freshly prepared by incubating pro-MMP-2 with 1 mM *p*-aminophenylmercuric acetate (dissolved in 200 mM Tris) for 30 min at 37 °C. Under these conditions, only the MMP-2 62-kDa species was detected by gelatin zymography. To isolate the MMP-9 82-kDa species, 1 mg of pro-MMP-9 was incubated

* This work was supported by National Institutes of Health Grant CA-61986 (to R. F.), a Wayne State University postdoctoral fellowship (to M. W. O.), and U. S. Army Grant DAMD17-97-1-7174 (to S. M.). The costs of publication of this article were defrayed in part by the payment of page charges. This article must therefore be hereby marked "advertisement" in accordance with 18 U.S.C. Section 1734 solely to indicate this fact.

|| To whom correspondence should be addressed: Dept. of Pathology, Wayne State University, 540 E. Canfield Ave., Detroit, MI 48201. Tel.: 313-577-1218; Fax: 313-577-8180; E-mail: rfridman@med.wayne.edu.

¹ The abbreviations used are: MMP, matrix metalloproteinase; TIMP, tissue inhibitor of metalloproteinase; PAGE, polyacrylamide gel electrophoresis; Me_2SO , dimethyl sulfoxide; CTD, C-terminal domain; SPR, surface plasmon resonance; MT1-MMP, membrane type 1-MMP.

with 20 μg of a recombinant catalytic domain of stromelysin 1 for 2 h at 37 °C. The sample was subjected to gelatin-agarose column chromatography to remove the stromelysin 1, and the fractions containing the 82-kDa activated MMP-9 were detected by gelatin zymography. The protein concentrations of the active species of MMP-2 (45 kDa) and MMP-9 (82 kDa) were determined by amino acid analysis or from their molar extinction coefficients (18). The MMP-2 (45 kDa) and MMP-9 (82 kDa) species were distributed in aliquots, flash frozen in liquid nitrogen, and stored at -80 °C. Both enzymes were stable for at least 12 months at -80 °C, as determined by gelatin zymography.

Recombinant human TIMP-2 was purified from media of infected HeLa cells as described (16), with the exception that instead of the CM-Sepharose matrix, the medium containing TIMP-2 was chromatographed on a Resource S column. TIMP-1 was purified by lectin lentil-Sepharose chromatography, as described (17). The TIMP-1-containing fractions were pooled, dialyzed against buffer HA to an ionic equivalent of less than 50 mM NaCl, and loaded onto a heparin-agarose column (5 ml) equilibrated with the same buffer. After the column was washed with HA buffer supplemented with 100 mM NaCl, TIMP-1 was eluted with a linear gradient of NaCl (200–400 mM) in HA buffer. The TIMP-1-containing fractions were pooled and dialyzed against phosphate-buffered saline. The protein concentrations of the recombinant TIMP-1 and TIMP-2 were determined using their molar extinction coefficients of 26,500 and 39,600 $\text{M}^{-1}\text{cm}^{-1}$, respectively (3). Purified TIMP-1 and TIMP-2 were distributed in aliquots, flash frozen in liquid nitrogen, and stored at -80 °C.

SDS-Polyacrylamide Gel Electrophoresis and Zymography—SDS-polyacrylamide gel electrophoresis (SDS-PAGE) was performed according to Laemmli (19). The proteins were visualized by staining overnight with a 0.25% solution of Coomassie Brilliant Blue R-250 in 45% methanol and 10% acetic acid and destaining in a solution of 20% methanol and 10% acetic acid. Zymography in a 10% SDS-PAGE containing 0.1% gelatin was performed as described (20).

Radioiodination of TIMPs—TIMP-1 and TIMP-2 were iodinated with carrier-free Na^{125}I (100 mCi/ml, Amersham Corp.) using IODO-GEN (Pierce). Briefly, glass vials were coated with 2 μg of IODO-GEN dissolved in 100% chloroform and dried with a stream of dry nitrogen. Twenty micrograms of either TIMP-1 or TIMP-2 were placed in an IODO-GEN-coated vial and allowed to incubate for 1 min at 25 °C. Na^{125}I (200 μCi) was added to each vial, and the iodination reaction was allowed to continue for 2 min at 25 °C. The reaction was stopped by the addition of bovine serum albumin (fraction V, Sigma) and NaI (Sigma) to final concentrations of 1 mg/ml and 1 mM, respectively. Unincorporated Na^{125}I was removed immediately using a 1-ml Sephadex-G50 (fine) spin column equilibrated in buffer C. The specific activity was determined by trichloroacetic acid-precipitable counts (>90% in the pellet), and the protein was quantitated by SDS-PAGE, Coomassie Blue staining of the gels, and densitometric scanning immediately after destaining. Densitometric analysis was performed using an AMBIS Image Analysis and Acquisition™ system (San Diego, CA) connected to a Dell 486/33 microcomputer equipped with the AMBIS Quant Probe™ software, version 4.01. The amount of ^{125}I -TIMPs was determined using known quantities of unlabeled purified TIMPs as standards electrophoresed in parallel. The specific activities of ^{125}I -TIMP-1 and ^{125}I -TIMP-2 were calculated to be 1.12 and 1.41 $\mu\text{Ci}/\mu\text{g}$, respectively.

Determination of Kinetic and Equilibrium Constants by SPR—TIMP-gelatinase interaction studies were performed using a Fison Iasys™ instrument. CM5™ research grade cells (Fison Iasys™) were used for all experiments. The carboxymethyl dextran matrix of the sensor cell was activated for 6 min using 0.2 ml of a mixture of 0.2 M 1-ethyl-3-(3-dimethylamino)propyl-carbodiimide and 0.05 M *N*-hydroxysuccinimide. After activation, the sensor cell was washed rapidly four times with 200 μl of buffer W followed by immediate immobilization of TIMP-1 and TIMP-2. Immobilization conditions were as follows: TIMP-1 (2 μg) or TIMP-2 (1 μg) was covalently coupled to the activated matrix in buffer B at a stirring rate of 50 for 9 min at 25 °C, followed by a single 200- μl wash with buffer B. The unreacted *N*-hydroxysuccinimide esters were quenched by a 200- μl injection of 0.1 M ethanolamine-HCl (pH 8.0). Finally, the sensor cell was washed with four 200- μl injections of buffer W. Under these conditions, 300 arc seconds of TIMP-1 and 400 arc seconds of TIMP-2 were immobilized. TIMP-gelatinase binding reactions were carried out in buffer W at a stirring speed of 50 at 25 °C. The cell was regenerated after gelatinase binding with a single 15-s pulse of 200 μl of 20 mM HCl. These regeneration conditions allowed for the retention of greater than 95% of the original TIMP binding capacity. The equilibrium constants (K_d) were calculated from the rate constants for association (k_a) and dissociation (k_d) from the equation $K_d = k_d/k_a$. For biphasic binding $K_d = k_d(2)/k_a(1)$ and $k_d(1)/k_a(2)$ for the low and

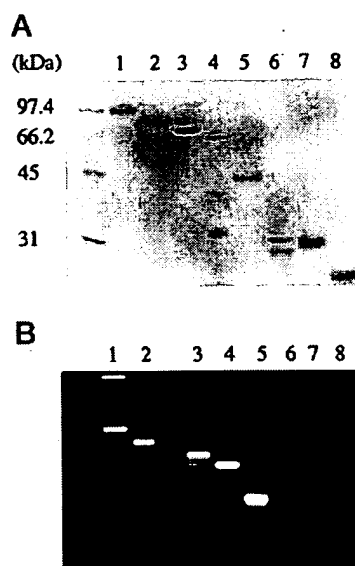


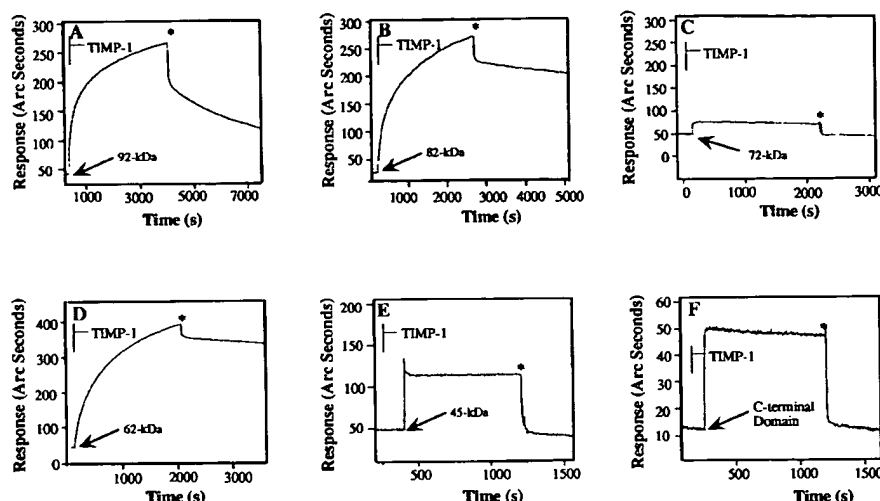
FIG. 1. SDS-PAGE and zymographic analysis of purified gelatinases and TIMPs. A, MMP-2 (latent and active species), MMP-9 (latent and active species), MMP-2 CTD, TIMP-1, and TIMP-2 were incubated for 120 min at 25 °C and subjected to 10% SDS-PAGE under reducing conditions. Proteins were detected by Coomassie Blue staining. Lane 1, pro-MMP-9 (2.5 μg). Lane 2, MMP-9 (82 kDa) (2 μg). Lane 3, pro-MMP-2 (2.5 μg). Lane 4, MMP-2 (62 kDa) (2.2 μg). Lane 5, MMP-2 (45 kDa) (2 μg). Lane 6, MMP-2 CTD (2 μg). Lane 7, TIMP-1 (3.5 μg). Lane 8, TIMP-2 (2 μg). B, MMP-2 and MMP-9 (latent and active species), MMP-2 CTD, TIMP-1, and TIMP-2 were incubated for 120 min at 25 °C and subjected to gelatin zymography. Lane 1, pro-MMP-9 (0.5 ng). Lane 2, MMP-9 (82 kDa) (0.15 ng). Lane 3, pro-MMP-2 (0.8 ng). Lane 4, MMP-2 (62 kDa) (0.2 ng). Lane 5, MMP-2 (45 kDa) (0.1 ng). Lane 6, MMP-2 CTD (100 ng). Lane 7, TIMP-1 (100 ng). Lane 8, TIMP-2 (115 ng).

high affinity binding sites, respectively. The binding constants for each analyte protein were determined in duplicate using at least five different concentrations of analyte (8.7–624 nM), in a final volume of 200 μl , where the response increased as a function of analyte concentration. For TIMP-1 pro-MMP-9 and MMP-9 (82 kDa) were both titrated from 10 to 200 nM; pro-MMP-2 and MMP-2 (62 kDa) were titrated from 20 to 250 and from 20 to 200 nM, respectively; MMP-2 (45 kDa) and the MMP-2 CTD were titrated from 55 to 440 and from 80 to 1250 nM, respectively. For TIMP-2 pro-MMP-9 and MMP-9 (82 kDa) were titrated from 100 to 420 and from 20 to 220 nM, respectively; pro-MMP-2 and MMP-2 (62 kDa) were titrated from 8.5 to 70 and from 10 to 120 nM, respectively; MMP-2 (45 kDa) and the MMP-2 CTD were titrated from 50 to 500 and from 15 to 330 nM, respectively. Furthermore, each analyte protein (200 nM) was subjected to analysis using a derivatized sensor cell to determine the amount of nonspecific binding to the carboxymethyl dextran matrix. In each case, less than a 7-arc second increase was observed. The binding curves were analyzed using the nonlinear data fitting program "Iasys Fafit™" using both monophasic and biphasic models to obtain the first-order association rate constant and the dissociation rate constant.

Binding of TIMPs to Gelatinases in Solution— ^{125}I -TIMP-1 or ^{125}I -TIMP-2 were incubated at 1:1 or 3:1 molar ratios with the latent and active forms of MMP-2 and MMP-9 for 30 min at 25 °C in buffer C. Binding reactions were carried out in 500 μl (final volume) where the concentration of the gelatinases was 25 nM or in 40 μl (final volume) where the concentration of enzymes was 450 nM. After binding, a 50- μl aliquot of gelatin-agarose matrix (a 50:50 slurry in buffer C) was added to each sample followed by incubation for 30 min at 25 °C. Each sample was centrifuged, washed three times with 400 μl of buffer C, and the resulting supernatant discarded. The radioactivity in the pellets was measured in a Packard 5650 gamma counter for 3 min. The amount of bound TIMP (pmol) was determined from the specific activity.

Gelatin-Agarose Chromatography of TIMP-Gelatinase Complexes—Pro-MMP-9 and pro-MMP-2 (200 pmol) were combined with TIMP-1 and TIMP-2 (600 pmol), respectively, in buffer C (final volume of 0.1 ml) and incubated for 40 min at 25 °C. These mixtures were then applied to a gelatin-agarose column (0.1 ml) and equilibrated with buffer C, and

FIG. 2. Sensorgrams of MMP-2 and MMP-9 binding to immobilized TIMP-1. Latent and active MMP-2 and MMP-9 species were allowed to bind to TIMP-1 and examined by SPR as described under "Experimental Procedures." A, pro-MMP-9 (92 kDa), 40 nM. B, MMP-9 (82 kDa), 40 nM. C, pro-MMP-2 (72 kDa), 250 nM. D, MMP-2 (62 kDa), 65 nM. E, MMP-2 (45 kDa), 440 nM. F, MMP-2 CTD, 625 nM. The asterisk indicates the end of the association phase.



the flow-through fraction was collected. The column was washed with 0.4 ml of buffer C, and 0.1-ml fractions were collected. The protein complexes were eluted with buffer C supplemented with 10% dimethyl sulfoxide (Me_2SO), and 0.1-ml fractions were collected. Twenty-five microliters of each fraction were analyzed by SDS-PAGE. Quantitation of the TIMPs and gelatinases in the complexes was determined by densitometric scanning of Coomassie Blue-stained gels, as described above, using known amounts of standard proteins.

Fluorometric Activity Assay for MMP-2 and MMP-9—The active forms of MMP-2 and MMP-9 were assayed for activity using the fluorescence quenching substrate MOAcPLGLA₂pr(Dnp)-AR-NH₂ (Peptide Institute, Inc., Japan, and first described by Knight *et al.* (21)). The peptide substrate was dissolved in 100% Me_2SO . Each assay was carried out at 25 °C in 2 ml (final volume) of 50 mM HEPES (pH 7.5), 150 mM NaCl, 5 mM CaCl_2 , 0.01% Brij-35, and Me_2SO (1% v/v), containing substrate and enzyme and/or inhibitor at the indicated concentrations. Substrate hydrolysis was monitored using a Spex Fluorolog 1681 (Spex Industries Inc.) fluorescence spectrophotometer with excitation and emission wavelengths set at 328 and 393 nm, respectively and controlled by an IBM-compatible computer using the dm3000 software provided by SPEXTM. The slit widths were maintained at 1 mm and the band pass was 3 nm. Fluorescent measurements were taken every 20 s with a 3-s integration time.

For the determination of the K_m and k_{cat} values of the MMP-2 and MMP-9 active species, the fluorescent substrate was used in the concentration range of 0.05 to 6.5 μM with 0.4 pmol (0.2 nM) of enzyme. The reaction was allowed to proceed for 6 min, and the initial velocity of each reaction was determined using the data collected up to 4 min. Three reaction rate determinations were made for each substrate concentration. The K_m and V_{max} values were determined by double-reciprocal analysis by linear regression using LINEST (Microsoft ExcelTM version 5.0).

To determine the association constants (k_{on}), the first-order binding constants were determined under the following conditions. The substrate concentration for each assay was 7 μM , a substrate concentration 2–4-fold greater than the experimentally determined K_m . TIMP-1 and TIMP-2 were added to the reaction, and the assay was initiated by addition of a 1 μM stock of enzyme to give a final concentration of 1 nM. The reaction was allowed to proceed for 10 min, and the rate of substrate cleavage was measured in triplicate for each TIMP concentration examined. For the MMP-2 45-kDa species, the concentrations of TIMP-1 and TIMP-2 were varied from 0 to 200 and from 0 to 100 nM, respectively. For the MMP-2 62-kDa species, both TIMP-1 and TIMP-2 were used in the concentration range of 0 to 30 nM. For the MMP-9 82-kDa species, TIMP-1 was used in the concentration range of 0 to 30 nM, and TIMP-2 was used in the concentration range of 0 to 60 nM. The first-order rate constant, k , was determined from the intersection point of the tangent to the curve at $t = \infty$ to the curve at $t = 0$ where $k = 1/t$, as described by Morrison and Walsh (22), where the data points gave equal increments of product formation as a function of time in the absence of inhibitor. The first-order rate constant, k , for each TIMP concentration was plotted as a function of TIMP concentration. The slope and error of the slope of this line gives the on-rate, k_{on} , and was determined by linear regression using LINEST (Microsoft ExcelTM v5.0).

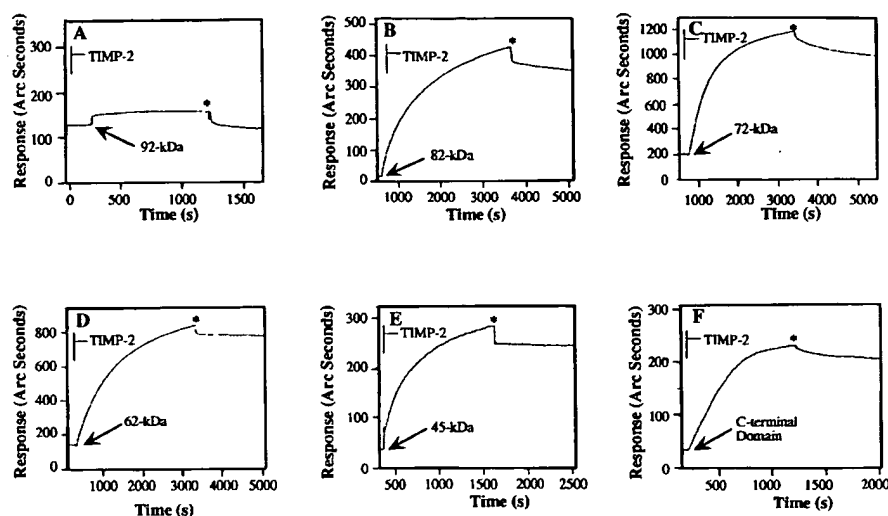
The dissociation constants (k_{off}) were determined in triplicate as follows. The MMP-2 45-kDa species was combined with TIMP-1 or TIMP-2 at a final concentration of 2 μM enzyme and 2.4 μM of either TIMP-1 or TIMP-2. The enzyme and inhibitor were allowed to incubate for 1 h at 25 °C. The k_{off} value of TIMP-1 and TIMP-2 for the MMP-2 (62 kDa) and MMP-9 (82 kDa) species were determined similarly, except that the enzyme and inhibitor were incubated at concentrations of 300 and 360 nM, respectively, for 1 h at 25 °C. The sample was added to the cuvette (final volume of 2 ml) containing 12 μM peptide substrate and a final concentration of 1 nM enzyme. The recovery of enzyme activity was followed for up to 40 min. The data were analyzed by the method of Glick *et al.* (23). The error of the slope of this line was determined by linear regression using LINEST (Microsoft ExcelTM version 5.0). The inhibition constants (K_i) were calculated by $K_i = k_{\text{off}}/k_{\text{on}}$.

RESULTS

Analysis of Purified Gelatinases and TIMPs—Determination of the binding constants for gelatinase-TIMP complexes requires pure enzymes and inhibitors. To this end, human recombinant latent and active MMP-2 and MMP-9 and TIMP-1 and TIMP-2 were purified to homogeneity. To address the role of the MMP-2 CTD and the catalytic site of MMP-2, we purified a C-terminally truncated MMP-2 45-kDa form (17) and obtained a purified recombinant CTD fragment (15). Fig. 1, A and B, demonstrates the purity and lack of any contaminating proteins in the samples used for kinetic analyses. Furthermore, active enzymes were not detected in the latent enzymes and vice versa (Fig. 1, A and B). Incubation of the enzymes for 120 min at 25 °C prior to electrophoresis confirmed their stability, an essential requirement for the SPR analysis.

SPR Analysis of Gelatinase-TIMP Interactions—The kinetic and equilibrium constants for gelatinase-TIMP interactions were determined by SPR (12–14) using a Fison IasysTM instrument. Since both TIMP-1 and TIMP-2 are acid stable (3), the inhibitors were chemically linked to the carboxymethyl dextran matrix on a sensor cell as described under "Experimental Procedures." Dilute solutions of latent or active MMP-2 or MMP-9 species (analytes) were allowed to bind to the immobilized TIMPs as a function of time. The results of typical binding assays are shown in the sensorgrams of Figs. 2 and 3. Only pro-MMP-9, active MMP-9 (82 kDa), and active MMP-2 (62 kDa) bound to TIMP-1 (Fig. 2, A, B, and D). In contrast, MMP-2 (latent and active forms), its CTD, and active MMP-9 bound to TIMP-2 (Fig. 3, B–F). The arc second "responses" observed with pro-MMP-2, the 45-kDa species, and the CTD to immobilized TIMP-1 (Fig. 2, C, E, and F) or with pro-MMP-9 to immobilized TIMP-2 (Fig. 3A), even at concentrations approaching 650 nM analyte, represent merely a change in the refractive index and not specific binding. The same refractive index change was

FIG. 3. Sensorgrams of MMP-2 and MMP-9 binding to immobilized TIMP-2. Latent and active MMP-2 and MMP-9 species were allowed to bind to TIMP-2 and examined by SPR as described under "Experimental Procedures." A, pro-MMP-9 (92 kDa), 205 nM. B, MMP-9 (82 kDa), 40 nM. C, pro-MMP-2 (72 kDa), 20 nM. D, MMP-2 (62 kDa), 20 nM. E, MMP-2 (45 kDa), 440 nM. F, MMP-2 CTD, 42 nM. The asterisk indicates the end of the association phase.



observed when the enzymes or domains thereof were allowed to bind to a sensor cell derivatized in the absence of TIMPs (data not shown).

SPR Analysis of Gelatinase-TIMP Interactions Reveal Low and High Affinity Sites—The association rate constant (k_a), dissociation rate constant (k_d), and equilibrium constant (K_d) of MMP-2 and MMP-9 forms for TIMP-1 and TIMP-2 were calculated from the data obtained from the Fison IasysTM analyses (Table I and Table II). To determine if the data fit the monophasic or biphasic models for nonlinear curve fitting, the following criteria were followed. First, random residuals for the nonlinear curve fitting of both the association and dissociation phases were required. Second, replotting of the \ln of the association phase *versus* time and of the \ln of the dissociation phase *versus* time was required to fit the theoretical plot provided by the software program Iasys FaspfitTM. Third, the root mean square deviation following nonlinear curve fitting for each model was required to be less than 1%. For the monophasic model, the root mean square deviation was consistently greater than 5% for the association and dissociation rate constant determinations. However, analysis of the data fit the biphasic model since it showed that the root mean square deviation value ranged between 0.001 and 0.38% for the first-order association rate constant and dissociation rate constant values. As shown in Tables I and II, these analyses indicated the existence of high and low affinity binding sites. The K_d values of TIMP-1 for the MMP-9 latent and active species were 35 and 23.9 nM for the high affinity site and 7.4 and 3.1 μ M for the low affinity site, respectively. Interestingly, the k_a and k_d values of TIMP-1 for the latent and active MMP-9 forms and the MMP-2 (62 kDa) active species were similar for both the high and low affinity sites (Table I). With TIMP-2, the K_d values for the latent and active MMP-2 species and the active MMP-9 were 5.2, 23.1, and 57.9 nM for the high affinity site and 0.19, 2.7, 12.7 μ M for the low affinity site, respectively (Table II). Binding of the active MMP-2 (45 kDa) species and the CTD to TIMP-2 only fit the monophasic model, where the root mean square deviation value was consistently less than 0.092% for the first-order association rate constant and dissociation rate constant values. This indicates a single binding site with K_d values of 315 and 61.6 nM, respectively (Table II). The lower K_d value for the TIMP-2-MMP-2 CTD complex suggests that the high affinity binding site resides within this domain.

Analysis of Gelatinase-TIMP Interactions in Solution—Previous studies suggested a 1:1 stoichiometry of gelatinase-TIMP complexes (9, 10, 24). Due to the nature of the SPR analysis

that requires immobilization of TIMPs, we examined the binding of gelatinases to the inhibitors in solution. To this end, unlabeled or radioiodinated TIMPs were allowed to bind to gelatinases, and the resultant complexes were analyzed by gelatin-agarose precipitation and gelatin-agarose chromatography. Binding of TIMP-1 and TIMP-2 to the latent and active forms of MMP-2 and MMP-9 was examined at concentrations at or near the K_d values for the high affinity site as determined by SPR using equimolar concentrations of enzymes and inhibitors. To account for the presence of the low affinity site, we also carried out similar experiments using a 3-fold molar excess inhibitor. Complex formation of the gelatinases and TIMPs at or near the K_d value for the high affinity site would be expected to reflect TIMP:gelatinase ratios of 0.5:1 and 1:1, whereas binding in the presence of excess TIMP would be expected to show a stoichiometry greater than 1:1 due to the low affinity site. Binding of equimolar and 3-fold molar excess of either ¹²⁵I-TIMP-1 (Fig. 4A) or ¹²⁵I-TIMP-2 (Fig. 4B) to pro-MMP-9, MMP-9 (82 kDa), pro-MMP-2, and MMP-2 (62 kDa) demonstrated a stoichiometry of 0.65–0.84:1 (equimolar) and 0.9–0.94:1 (3-fold molar excess), indicating a 1:1 stoichiometry. Under the same conditions, the active MMP-2 (45 kDa) species showed no detectable binding to either TIMP-1 or TIMP-2 in agreement with the K_d value determined by SPR (Table II). Since the SPR data indicated the existence of a low affinity site with K_d values in the micromolar range (Tables I and II), we asked whether the stoichiometry of the enzyme-inhibitor complex could be forced to a ratio approaching 1:2 in solution. To this end, binding was carried out at concentrations of enzyme and inhibitor 20-fold greater than the K_d for the high affinity site and at either equimolar ratios or 3-fold molar excess inhibitor. Fig. 4, C and D, shows that at 1:1 molar ratios, the stoichiometry is 1:1, as expected from the K_d values determined by SPR. Under conditions of 3-fold molar excess inhibitor, gelatin-agarose precipitation experiments showed an increase in ¹²⁵I-TIMP binding to the enzymes with enzyme:inhibitor ratios of 1:1.4 to 1:1.8. In addition, coprecipitation of ¹²⁵I-TIMP-2 was observed with the active MMP-2 (45 kDa) species, consistent with a ~1:1 stoichiometry (Fig. 4D). In contrast, ¹²⁵I-TIMP-1 failed to coprecipitate with the 45-kDa species, regardless of the enzyme and TIMP concentrations used (Fig. 4, A and C).

Analysis of the stoichiometry of pro-MMP-2-TIMP-2 and pro-MMP-9-TIMP-1 complexes was also performed by densitometric analysis of SDS-polyacrylamide gels of enzyme-inhibitor complexes subjected to gelatin-agarose chromatography, as de-

TABLE I
Kinetic and equilibrium constants of gelatinase forms with TIMP-1 determined by SPR analysis

The errors for the k_a and k_d rate constants are expressed as the standard deviation of the slope and the standard deviation of five analyte concentrations, respectively, from two separate experiments. The errors for the K_d values represent the sum of the errors from the k_a and k_d values.

Analyte protein	k_a (1)	k_a (2)	k_d (1)	k_d (2)	K_d	K_d
	$M^{-1} s^{-1} \times 10^{-3}$		$s^{-1} \times 10^3$		μM	nM
MMP-9 species						
92 kDa	34.2 ± 0.2	4.0 ± 0.3	29.7 ± 3.9	1.2 ± 0.2	7.4 ± 0.9	35.0 ± 5.8
82 kDa	51.8 ± 0.1	7.4 ± 0.3	23.0 ± 3.2	1.2 ± 0.2	3.1 ± 0.4	23.9 ± 3.8
MMP-2 species						
72 kDa	NB ^a	NB	NB	NB		
62 kDa	44.0 ± 0.3	4.0 ± 0.7	33.9 ± 2.9	1.3 ± 0.2	8.5 ± 0.7	28.6 ± 4.5
45 kDa	NB	NB	NB	NB		
CTD	NB	NB	NB	NB		

^a NB, no binding.

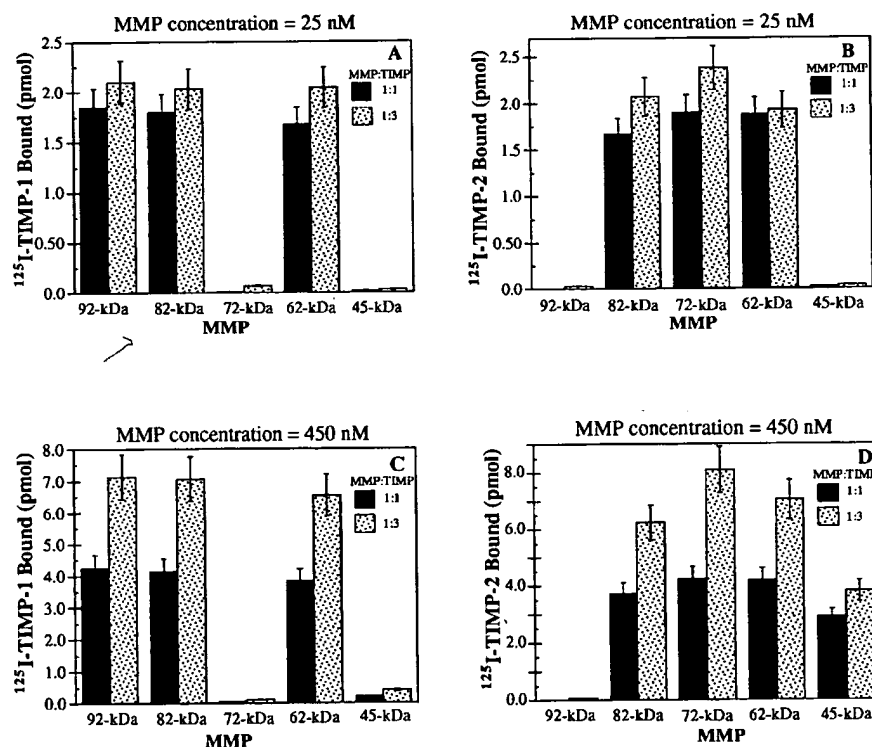
TABLE II
Kinetic and equilibrium constants of gelatinase forms with TIMP-2 determined by SPR analysis

The errors for the k_a and k_d rate constants are expressed as the standard deviation of the slope and the standard deviation of five analyte concentrations, respectively, from two separate experiments. The errors for the K_d values represent the sum of the errors from the k_a and k_d values.

Analyte protein	k_a (1)	k_a (2)	k_d (1)	k_d (2)	K_d	K_d
	$M^{-1} s^{-1} \times 10^{-3}$		$s^{-1} \times 10^3$		μM	nM
MMP-9 species						
92 kDa	NB ^a	NB	NB	NB		
82 kDa	22.8 ± 0.2	2.6 ± 0.2	33.1 ± 3.5	1.3 ± 0.2	12.7 ± 1.3	57.9 ± 7
MMP-2 species						
72 kDa	140.6 ± 0.6	24.7 ± 1.9	4.7 ± 0.4	0.7 ± 0.1	0.19 ± 0.02	5.2 ± 0.4
62 kDa	32.6 ± 0.3	4.8 ± 0.8	12.7 ± 0.6	0.8 ± 0.1	2.7 ± 0.1	23.1 ± 4.1
45 kDa	3.2 ± 0.2		1.0 ± 0.1			315 ± 34
CTD	92.1 ± 3.9		5.7 ± 0.9			61.6 ± 11

^a NB, no binding.

FIG. 4. Coprecipitation of gelatinase-TIMP complexes. ^{125}I -TIMP-1 and ^{125}I -TIMP-2 were allowed to bind to MMP-9 (latent and active species) and to MMP-2 (latent and active species) for 30 min at 25 °C, and the resulting complexes were subjected to precipitation with gelatin-agarose as described under "Experimental Procedures." A, gelatinases (25 nM) incubated with 25 nM (solid bars) or 75 nM (dotted bars) ^{125}I -TIMP-1. B, gelatinases (25 nM) incubated with 25 nM (solid bars) or 75 nM (dotted bars) ^{125}I -TIMP-2. C, gelatinases (450 nM) incubated with 450 nM (solid bars) or 1.4 μM (dotted bars) ^{125}I -TIMP-1. D, gelatinases (450 nM) incubated with 450 nM (solid bars) or 1.4 μM (dotted bars) ^{125}I -TIMP-2. The error bars represent the standard deviation from three independent determinations.



scribed under "Experimental Procedures." Densitometric analysis of the gels depicted in Fig. 5, A and B, revealed a stoichiometry ranging from 1.4:1 to 1.5:1 for the TIMP-1-pro-MMP-9 complex and from 1.5:1 to 1.6:1 for the TIMP-2-pro-MMP-2 complex (data not shown). Thus, at micromolar concentrations

of enzyme and an excess of inhibitor, a second TIMP molecule can bind to the proenzyme form, in agreement with the data obtained by the coprecipitation experiments.

Catalytic Competence of Active Gelatinases—Previous studies reported "apparent" K_i values of TIMP-1 and TIMP-2 for

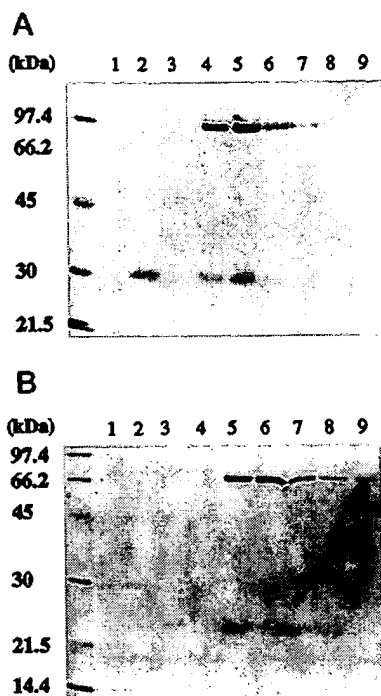


FIG. 5. Gelatin-agarose chromatography of gelatinase-TIMP complexes. A, TIMP-1 (600 pmol) and pro-MMP-9 (200 pmol) were allowed to complex for 40 min at 25 °C and subjected to gelatin-agarose column chromatography followed by 10% SDS-PAGE under reducing conditions as described under "Experimental Procedures." Proteins were detected by Coomassie Blue staining: lane 1, wash fraction number 1; lane 2, wash fraction number 2; lane 3, wash fraction number 3; lane 4, elution fraction 1; lane 5, elution fraction 2; lane 6, elution fraction 3; lane 7, elution fraction 4; lane 8, elution fraction 5; lane 9, elution fraction 6. B, same as in A except that TIMP-2 (600 pmol) and pro-MMP-2 (200 pmol) were subjected to 12% SDS-PAGE. Lane 1, wash fraction number 1; lane 2, wash fraction number 2; lane 3, wash fraction number 3; lane 4, wash fraction number 4; lane 5, elution fraction 1; lane 6, elution fraction 2; lane 7, elution fraction 3; lane 8, elution fraction 4; lane 9, elution fraction 5.

MMP-2 and MMP-9 in the picomolar range (9, 10, 25). Since K_d is equal to K_i , when inhibition is studied, the data derived from SPR analysis indicated K_i values in the nanomolar range. Therefore, binding and affinity of the TIMPs for the gelatinases were evaluated using enzymatic activity assays with the peptide substrate MOAcPLGLA₂pr(Dnp)-AR-NH₂ (21). As shown in Fig. 6A, the enzymes show saturation kinetics in hydrolysis of the peptide substrate. Double-reciprocal analysis of the data (Fig. 6B) allowed for determination of the K_m , k_{cat} , and k_{cat}/K_m values (Table III). Insofar as K_m may approximate K_s , and as such give an expression of affinity, these enzymes show essentially the same affinity for the substrate with K_m values in the range of 1.5 to 3 μ M. In addition, the correlation coefficient (r^2) values for the fitted lines are ~ 0.99 (Fig. 6B). Thus, the results indicate that all these enzymes are equally competent as catalysts in hydrolysis of the synthetic substrate with k_{cat}/K_m values equivalent to or greater than values obtained previously (10, 11).

Enzymatic Determination of the Inhibition Constant of TIMP-1 and TIMP-2 for the Gelatinases—We examined the binding of TIMP-1 and TIMP-2 to the active forms of MMP-2 and MMP-9 by enzyme inhibition assays as described under "Experimental Procedures." As shown in Fig. 7, TIMP-1 and TIMP-2 inhibit each enzyme. However, TIMP-1 failed to inhibit the active MMP-2 (45 kDa) species even at concentrations of 200 nM (Fig. 7A). The pattern of inhibition was consistent with a slow binding process (22). This type of behavior is character-

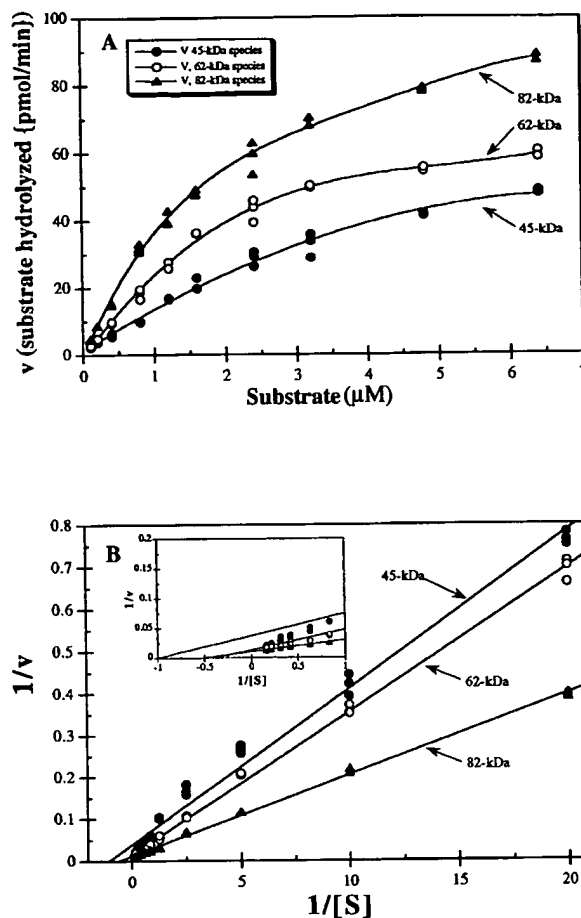


FIG. 6. Initial velocity and double-reciprocal analysis for MMP-2 and MMP-9 active forms for MOAcPLGLA₂pr(Dnp)-AR-NH₂ hydrolysis. A, initial rates were determined by the fluorescence peptide assay. Each assay was performed in triplicate, contained 0.4 pmol (0.2 nM) of enzyme, and was allowed to proceed for 6 min as described under "Experimental Procedures." B, Lineweaver-Burk Plot of the data from A. The inset in B represents a magnification of the substrate concentrations between 1.25 and 6.5 μ M. Open circles, MMP-2 62-kDa species; closed circles, MMP-2 45-kDa species; closed triangles, MMP-9 82-kDa species.

TABLE III
Enzymatic parameters for the hydrolysis of MOAcPLG-A₂pr(DNP)-AR-NH₂ by gelatinases

The error is expressed as the standard deviation of the intercepts from three data sets.

Enzyme	K_m μ M	k_{cat} s^{-1}	k_{cat}/K_m $M^{-1} s^{-1}$
MMP-9, 82 kDa	2.46 ± 0.34	4.41 ± 0.55	$(17.9 \pm 0.2) \times 10^5$
MMP-2, 62 kDa	3.06 ± 0.74	3.18 ± 0.46	$(10.4 \pm 0.2) \times 10^5$
MMP-2, 45 kDa	1.52 ± 0.29	1.30 ± 0.21	$(8.6 \pm 1.6) \times 10^5$

ized by the formation of curves that display a time-dependent onset of inhibition within the period that substrate turnover is linear in the absence of inhibitor. For slow binding inhibition, the first-order rate constant (k) is equal to the rate of product formation that is derived from the asymptote, where the k value is determined from the intersection point of the tangent to the curve at $t = 0$, as given by the expression $P = v_0 t$. The asymptote of the curve is given by the equation $P = v_s t + (v_0 - v_s)/k$. At this point, $k = 1/t$ (22). The association rate constant (k) for the formation of enzyme-inhibitor complexes is determined from these progress curves of substrate hydrolysis. The second-order rate constant (k_{on}) is provided by linear regres-

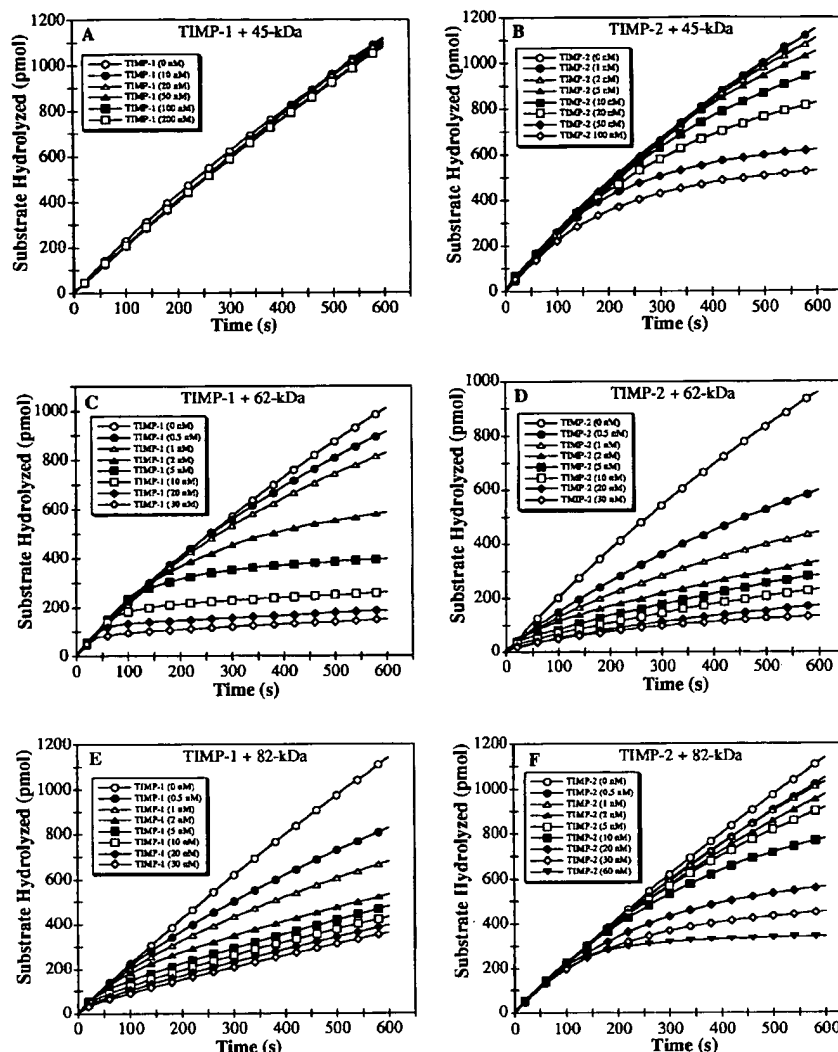


FIG. 7. Slow binding inhibition of gelatinases by TIMP-1 and TIMP-2. The active species of MMP-2 and MMP-9 (1 nM) were assayed with increasing concentrations of TIMP-1 and TIMP-2 as described under "Experimental Procedures." A, C, and E, TIMP-1 with MMP-2 (45 kDa), MMP-2 (62 kDa), and MMP-9 (82 kDa), respectively. B, D, and F, TIMP-2 with MMP-2 (45 kDa), MMP-2 (62 kDa), and MMP-9 (82 kDa), respectively.

sion of k as a function of inhibitor concentration. The off-rate (k_{off}) was determined by the recovery of enzyme activity (Fig. 8).

Tables IV and V show the k_{on} and k_{off} values using the analysis described above. TIMP-1 inhibits both MMP-9 (82 kDa) and MMP-2 (62 kDa) enzymes with comparable rate constants for inhibition onset (k_{on}) and recovery of activity (k_{off}), and by consequence result in similar K_i values (8.5 and 9.7 nM, respectively). The k_{on} is fast ($>10^5 \text{ M}^{-1} \text{ s}^{-1}$) and k_{off} is slow ($\sim 10^{-3} \text{ s}^{-1}$), resulting in effective inhibition. The same trend is true for TIMP-2 with MMP-9 (82 kDa) and MMP-2 (62 kDa) enzymes (K_i values of 43.4 and 7.2 nM, respectively). For the active MMP-2 (45 kDa) species, the k_{on} ($1.4 \times 10^4 \text{ M}^{-1} \text{ s}^{-1}$) was considerably slower resulting in a K_i value of 275 nM, indicative of a relatively poor affinity of the inhibitor for the truncated enzyme. The k_{on} values (Tables IV and V) of TIMP-1 for MMP-2 (62 kDa) and MMP-9 (82 kDa) and of TIMP-2 for MMP-2 (62 and 45 kDa) and MMP-9 (82 kDa) species were consistently greater (2.5 to 7-fold) than those determined by SPR (Tables I and II). Likewise, the k_{off} values (Tables IV and V) were 1.5 to 3-fold higher than those determined by SPR (Tables I and II). The calculated K_i values of TIMP-1 and TIMP-2 for the MMP-2 (62 and 45 kDa) and MMP-9 (82 kDa) (Tables IV and V) species were in the nanomolar range and within 3-fold of the K_d values determined by SPR (Tables I and II).

DISCUSSION

We have carried out a comprehensive study to determine the kinetic parameters for the binding of TIMP-1 and TIMP-2 to the latent and active forms of MMP-2 and MMP-9. The results of the SPR analyses were consistent with previous studies (4, 5, 9–11) demonstrating binding of TIMP-1 to the latent and active MMP-9 and MMP-2 (62 kDa) species, and binding of TIMP-2 to the latent and active MMP-2 species, and the active form of MMP-9 (82 kDa). In addition, TIMP-1 and TIMP-2 failed to interact with pro-MMP-2 and pro-MMP-9, respectively (for reviews see Refs. 2 and 3), as expected. We have also shown that TIMP-1, in contrast to TIMP-2, did not bind to the CTD of MMP-2 or to the MMP-2 45-kDa species. SPR methodology for analysis of TIMP-MMP interactions was used in a previous study by Bodden *et al.* (26) which demonstrated k_a , k_d , and K_d values of $8.9 \times 10^4 \text{ M}^{-1} \text{ s}^{-1}$, $3.6 \times 10^{-4} \text{ s}^{-1}$, and 4.1 nM, respectively, for the complex of TIMP-1 with active MMP-1. The K_d values of the MMP-1/TIMP-1 interaction (determined by SPR) are 7- and 14-fold lower than those for TIMP-1 with the active MMP-9 (82 kDa) and MMP-2 (62 kDa) species, respectively, as reported here. This suggests that TIMP-1 may be a more efficient inhibitor of MMP-1 than of MMP-9 and MMP-2.

Previous studies demonstrated that binding of TIMP-1 and

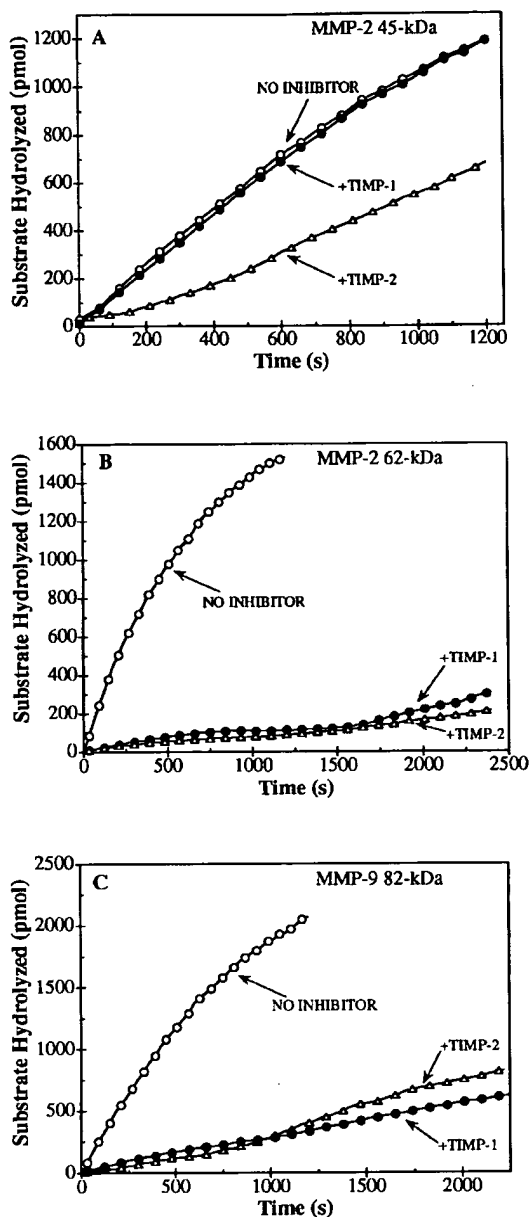


FIG. 8. Dissociation of the MMP-2 and MMP-9 active species from TIMP-1 and TIMP-2. The active species of MMP-2 and MMP-9 were preincubated with TIMP-1 and TIMP-2, and then the recovery of activity was monitored as described under "Experimental Procedures." Open circles, enzymes without TIMPs; closed circles, enzymes with TIMP-1; and open triangles, enzymes with TIMP-2. A, substrate hydrolysis by active MMP-2 (45 kDa). B, substrate hydrolysis by active MMP-2 (62 kDa). C, substrate hydrolysis by active MMP-9 (82 kDa).

TIMP-2 to MMP-9 and MMP-2 is mediated by two distinct domains of the inhibitor molecules and two domains of the enzymes (3, 9–11, 25, 27). The N-terminal domains of TIMPs were shown to bind to the enzymes within the active site domain, and the C-terminal regions of TIMPs were shown to bind to the C-terminal domain of the enzyme. Consistent with this model, we have found biphasic binding kinetics of TIMP-1 for MMP-9 (the latent and active forms) and MMP-2 (62 kDa) active form and of TIMP-2 for active MMP-9 (82 kDa) and MMP-2 (72- and 62-kDa species) that were indicative of the existence of high and low affinity binding sites. This was further supported by the results with the CTD of MMP-2 and the MMP-2 (45 kDa) species that, in contrast to pro-MMP-2 and

TABLE IV
Association, dissociation and inhibition constants for gelatinase/TIMP-1 interactions

The errors for the k_{on} and k_{off} values are expressed as the deviation of the slopes. The error for K_i value is the sum of the error from the k_{on} and k_{off} values.

Enzyme	k_{on} $M^{-1} s^{-1} \times 10^{-5}$	k_{off} $s^{-1} \times 10^3$	K_i nM
MMP-9, 82 kDa	2.48 ± 0.47	2.1 ± 1.1	8.5 ± 2.9
MMP-2, 62 kDa	2.46 ± 0.17	2.4 ± 0.7	9.7 ± 1.7
MMP-2, 45 kDa	NB ^a	NB	NB

^a NB, no binding.

TABLE V
Association, dissociation and inhibition constants for gelatinase/TIMP-2 interactions

The errors for the k_{on} and k_{off} values are expressed as the deviation of the slopes. The error for K_i value is the sum of the error from the k_{on} and k_{off} values.

Enzyme	k_{on} $M^{-1} s^{-1} \times 10^{-5}$	k_{off} $s^{-1} \times 10^3$	K_i nM
MMP-9, 82 kDa	0.57 ± 0.03	2.5 ± 0.6	43.4 ± 7.4
MMP-2, 62 kDa	2.23 ± 0.64	1.6 ± 0.6	7.2 ± 2.5
MMP-2, 45 kDa	$0.14 \pm .01$	3.8 ± 0.5	275 ± 31.1

active MMP-2 (62 kDa), showed monophasic binding kinetics with TIMP-2. Thus, the data obtained with the 45-kDa species and the CTD suggest that the latter contains the high affinity site, whereas the lower affinity binding site resides within the catalytic domain. SPR analysis of the 45-kDa species also suggested the contribution of the CTD for the binding of TIMP-2 to the low affinity site. Indeed, the K_d value describing the affinity of TIMP-2 for the 45-kDa species (315 nM) was 8.5-fold lower than that for the low affinity site of TIMP-2 for the MMP-2 62-kDa form (2.7 μM), which presumably resides within the catalytic domain. Thus, removal of the CTD appears to increase the affinity of TIMP-2 for the catalytic domain. Alternatively, the low affinity site in the MMP-2 62-kDa enzyme may be different from that in the 45-kDa species, and its accessibility is only possible after removal of the CTD. The lack of any measurable binding of TIMP-1 to both the 45-kDa active species and the CTD were unexpected since the 62-kDa form bound TIMP-1 with high affinity. Since the binding of the 62-kDa species to TIMP-1 also showed biphasic binding, it is possible that the CTD of MMP-2 may work synergistically with the active site in promoting TIMP-1 binding.

The contribution of the N-terminal prodomain of the gelatinases for the binding of TIMPs was also made apparent by the SPR analysis, particularly with MMP-2. Here, removal of the N-terminal prodomain resulted in a decreased affinity of TIMP-2 for the active (62 kDa) form, at both the low (14-fold reduction) and high affinity (5-fold reduction) sites. In contrast, this effect was less apparent with MMP-9 and TIMP-1. The affinity of TIMP-1 to both the low and high affinity sites for pro-MMP-9 and active MMP-9 varied by approximately 2-fold. Nevertheless, it was interesting to observe biphasic binding of TIMP-1 to pro-MMP-9 since the N-terminal prodomain has been suggested to preclude pro-MMP-9/TIMP-1 interaction at sites other than the CTD (3, 10). Thus, the SPR data suggest that TIMP-1 may also bind to a site different than the CTD of pro-MMP-9.

The biphasic binding observed by SPR agreed with data obtained in the solution binding experiments and were consistent with a 1:1 stoichiometry. These studies also showed that latent and active gelatinase forms, except for the 45-kDa MMP-2 species, can bind a second TIMP molecule under conditions of excess inhibitor and at micromolar concentrations.

We have also observed that binding of gelatinases to the TIMPs, at concentrations near or below the K_d values, for the high affinity sites showed sub-stoichiometric enzyme-inhibitor complexes consistent with K_d values in the nanomolar range. Likewise, binding at concentrations greater than the K_d values for the high affinity sites resulted in the generation of near-stoichiometric complexes. Taken together, these data suggest that the two sites of interaction are unique and can bind inhibitor independently. It is difficult to envision the evolutionary reason for conservation of the second TIMP binding site, if it were irrelevant *in vivo*. The existence of the second site awaits resolution of the crystal structures of the gelatinase-TIMP complexes. Furthermore, regarding pro-MMP-2, the interaction of this enzyme with TIMP-2 will have to be addressed in the context of a current model describing the association of pro-MMP-2 with a MT1-MMP-TIMP-2 complex (7).

We determined the k_{on} , k_{off} , and K_i values by enzyme inhibition analysis and demonstrated that both TIMP-1 and TIMP-2 behave as slow binding inhibitors. Using kinetic treatment for slow binding inhibition (22), the results indicated that the association of TIMPs and gelatinases is rapid ($k_{on} \sim 10^5 \text{ M}^{-1} \text{ s}^{-1}$). Furthermore, the dissociation of the enzyme-inhibitor complexes was slow ($k_{off} \sim 10^{-3} \text{ s}^{-1}$), resulting in a very effective inhibition of activity. The k_{off} values were determined from recovery of enzyme activity as a function of time, which allowed for the determination of the K_i value. This value was calculated to be in the nanomolar range, similar to the results obtained by the SPR analysis. Also, in agreement with the SPR results, the enzyme-inhibition studies demonstrated that the 45-kDa species of MMP-2 exhibited a 35-fold reduction in affinity (275 nM) for TIMP-2 when compared with the 62-kDa enzyme. Similar to these results, Taylor *et al.* (28) showed a 10–20-fold decrease in the affinity (247 nM) of TIMP-1 for a C-terminally truncated MMP-1 as opposed to the full-length active enzyme. Collectively, these findings support the importance of the C-terminal domain for the effective inhibition by TIMPs among distinct members of the MMP family.

Previous studies determined that the K_i values of TIMP-1 and TIMP-2 for MMP-2 and MMP-9 are in the $\leq 10^{-9} \text{ M}$ range (9, 10, 25). However, these K_i values were reported as apparent in nature (9, 10). Nevertheless, these values are 3–4 orders of magnitude lower than the K_d and K_i values reported herein using SPR and enzyme-inhibition studies, respectively. This discrepancy may be due to differences in the following: (i) substrate (0.5 μM , Ref. 9, *versus* 7 μM); (ii) enzyme (0.05 nM, Ref. 9, *versus* 1 nM); and (iii) inhibitor (0.1 nM, Ref. 9, *versus* 0.5–30 nM) concentrations for association rate determinations; and (iv) differences in enzyme and inhibitor concentrations used in the determination of the dissociation rate constants (0.002 nM, Ref. 9, *versus* 1 nM). Furthermore, regarding the MMP-9-TIMP-1 complex, k_{off} values were not determined; thus, K_i values could not be obtained (10). Our data, however, are in close agreement with the SPR analysis and the enzyme inhibition studies performed by others. Yu *et al.*² recently reported that pro-MMP-2 binds to immobilized TIMP-2 with biphasic kinetics and with a K_d value of $\sim 4 \text{ nM}$. Also, Bodden *et al.* (26) reported K_d values of 4.1 nM by SPR analysis for a complex of active MMP-1 with TIMP-1, and Taylor *et al.* (28) reported K_d values of ~ 20 and 8 nM for MMP-1 with TIMP-1 by enzyme inhibition studies.

It is significant that the SPR analysis, which evaluates protein-protein interactions without regard for inhibition of enzymatic activity, indicated biphasic behavior and provided K_d values for the high affinity site similar to the K_i values determined from enzyme inhibition assays. The fact that the kinetics of inhibition are monophasic clearly indicates that one binding event accounts for the onset of enzymatic inhibition. However, the presence of a second gelatinase-TIMP interaction site in the latent and active forms was clearly evident in the SPR experiments with the 45-kDa species of MMP-2 and the CTD fragment. The role of the second site in manifestation of enzyme inhibition is unclear. We wish to underscore that the kinetic parameters for enzyme inhibition corresponded closely (within 3-fold) to those for the high affinity phase of the protein-protein interaction determined by SPR analysis. Thus, two entirely distinct analyses provided essentially similar results. The ultimate structural information should await elucidation of the crystal structures for the gelatinases and gelatinase-inhibitor complexes.

Acknowledgments—We are indebted to Drs. Steven Ledbetter and Roger Poorman (Pharmacia-Upjohn) for their assistance with the use of the Fison IasysTM instrument, to Dr. G. I. Goldberg (Washington University, St. Louis, MO) for providing the CTD of MMP-2, and to Dr. Paul Cannon (Center for Bone and Joint Research, Palo Alto, CA) for the human stromelysin 1.

REFERENCES

- Matrisian, L. (1990) *Trends Genet.* **6**, 121–125
- Murphy, G., and Crabbe, T. (1995) *Methods Enzymol.* **248**, 470–484
- Murphy, G., and Willenbrock, F. (1995) *Methods Enzymol.* **248**, 496–510
- Goldberg, G. I., Marmer, B. L., Grant, G. A., Eisen, A. Z., Wilhelm, S., and He, C. (1989) *Proc. Natl. Acad. Sci. U. S. A.* **86**, 8207–8211
- Wilhelm, S. M., Collier, I. E., Marmer, B. L., Eisen, A. Z., Grant, G. A., and Goldberg, G. I. (1989) *J. Biol. Chem.* **264**, 17213–17221
- Will, H., Atkinson, S. J., Butler, G. S., Smith, B., and Murphy, G. (1996) *J. Biol. Chem.* **271**, 17119–17123
- Strongin, A. Y., Collier, I., Bannikov, G., Marmer, B. L., Grant, G. A., and Goldberg, G. I. (1995) *J. Biol. Chem.* **270**, 5331–5338
- Pei, D., and Weiss, S. J. (1996) *J. Biol. Chem.* **271**, 9135–9140
- Willenbrock, F., Crabbe, T., Slocumbe, P. M., Sutton, C. W., Docherty, A. J. P., Cockett, M. I., O'Shea, M., Brocklehurst, K., Phillips, I. R., and Murphy, G. (1993) *Biochemistry* **32**, 4330–4337
- O'Connell, J. P., Willenbrock, F., Docherty, A. J. P., Eaton, D., and Murphy, G. (1994) *J. Biol. Chem.* **269**, 14967–14973
- Nguyen, Q., Willenbrock, F., Cockett, M. I., O'Shea, M., Docherty, A. J. P., and Murphy, G. (1994) *Biochemistry* **33**, 2089–2095
- O'Shannessy, D. J., Brigham-Burke, K., Soneson, K., Hensley, P., and Brooks, I. (1994) *Methods Enzymol.* **240**, 323–349
- Karlsson, R., Michealsson, A., and Mattsson, L. (1991) *J. Immunol. Methods* **145**, 229–240
- Malmqvist, M. (1993) *Nature* **361**, 186–187
- Lisbon, A. M., Gittis, A. G., Collier, I. E., Marmer, B. L., Goldberg, G. I., and Lattman, E. E. (1995) *Nat. Struct. Biol.* **11**, 938–942
- Fridman, R., Fuerst, T. R., Bird, R. E., Hoyhtya, M., Oelkelt, T. M., Kraus, S., Komarek, D., Liotta, L. A., Berman, M. L., and Stetler-Stevenson, W. G. (1992) *J. Biol. Chem.* **267**, 15398–15405
- Fridman, R., Toth, M., Peña, D., and Mobashery, S. (1995) *Cancer Res.* **55**, 2548–2555
- Gill, S. C., and von Hippel, P. H. (1989) *Anal. Biochem.* **182**, 319–326
- Laemmli, U. K. (1970) *Nature* **227**, 680–685
- Brown, P. T., Levey, A. T., Margulies, I. M. K., Liotta, L. A., and Stetler-Stevenson, W. G. (1990) *Cancer Res.* **50**, 6184–6191
- Knight, C. G., Willenbrock, F., and Murphy, G. (1992) *FEBS Lett.* **296**, 263–266
- Morrison, J. F., and Walsh, C. T. (1988) *Adv. Enzymol. Relat. Areas Mol. Biol.* **61**, 201–301
- Glick, B. R., Brubacher, L. J., and Leggett, D. J. (1978) *Can. J. Biochem.* **56**, 1055–1057
- Stetler-Stevenson, W. G., Krutzsch, H. C., and Liotta, L. A. (1989) *J. Biol. Chem.* **264**, 17374–17378
- Murphy, G., Willenbrock, F., Ward, R. V., Cockett, M. I., Eaton, D., and Docherty, A. J. P. (1992) *Biochem. J.* **283**, 637–641
- Bodden, M. K., Harber, G. J., Birkedal-Hansen, B., Windsor, L. J., Caterina, N. C. M., Engler, J. A., and Birkedal-Hansen, H. (1994) *J. Biol. Chem.* **269**, 18943–18952
- Murphy, G., Houbrechts, A., Cockett, M. I., Williamson, R. A., O'Shea, M., and Docherty, A. J. P. (1991) *Biochemistry* **30**, 8097–8102
- Taylor, K. B., Windsor, J., Caterina, N. C. M., Bodden, M. K., and Engler, J. A. (1996) *J. Biol. Chem.* **271**, 23938–23945

² Yu, A. E., Fisher, R. J., Kleiner, D. E., and Stetler-Stevenson, W. G. (1996) Abstract from the Inhibitors of Metalloproteinases in Development and Disease TIMPs, September 25–29, 1996, Banff, Alberta, Canada.